PROCEEDINGS OF SCIENCE

Status and expected performance of the AugerPrime Radio Detector

Jannis Pawlowsky[a,*] **for the Pierre Auger**[b] **collaboration**

[a] *Bergische Universität Wuppertal, Gaußstraße 20, 42119, Wuppertal, Germany*
[b] *Observatorio Pierre Auger, Av. San Martín Norte 304, 5613 Malargüe, Argentina*
Full author list: https://www.auger.org/archive/authors_icrc_2023.html

E-mail: spokespersons@auger.org

The ongoing AugerPrime upgrade of the Pierre Auger Observatory will yield sensitivity and precision for measuring ultra-high energy (UHE) cosmic rays that are significantly improved over the baseline design. A key part is the installation of the Radio Detector (RD), consisting of loop antennas mounted on top of each of the 1660 water-Cherenkov detectors (WCD). These antennas, with polarizations both parallel and perpendicular to Earth's magnetic field, are sensitive to inclined air showers and will also improve the sky coverage and exposure of the observatory. Of special interest is the great sensitivity to the electromagnetic component of air showers, yielding new information for the reconstruction of the primary mass, energy and arrival direction. Complementing traditional particle detectors like the WCD, the combination of both yields new opportunities to detect rare primary particles, e.g. UHE photons and neutrinos with a large identification probability.

Here we present the status and future prospects of the RD. With mass production and deployment ongoing, we show air shower statistics and reconstructions of the already installed detector stations. We detail the layout and integration of the RD, demonstrating the potential of the observatory including radio measurements and RD triggering, especially to detect air showers with weak particle footprints. We show that the new trigger enables the measurement of events for which traditional particle detectors are less sensitive.

38th International Cosmic Ray Conference (ICRC2023)
26 July - 3 August, 2023
Nagoya, Japan

*Speaker

PoS(ICRC2023)344

1. Introduction

The Pierre Auger Observatory is the largest detector for measuring ultra-high energy cosmic rays (UHECR). The observatory consists of 4 fluorescence telescope sites (FD) and 1660 water-Cherenkov detectors (WCDs) covering an area of $\approx 3\,000\,\mathrm{km}^2$. While most of the WCDs are ordered in a triangular grid with 1.5 km spacing, a smaller area with 61 WCDs has a spacing of 750 m and 433 m. This area has a large overlap with the Auger Engineering Radio Array (AERA) [1], which consists of 150 radio antennas covering an area of $17\,\mathrm{km}^2$. The combination of all detectors makes the Pierre Auger Observatory the most sensitive detector for detecting UHECR and other rare and presumed particles like ultra-high energy neutrinos and photons.

In order to further increase the trigger efficiency, mass sensitivity and exposure of the observatory, the AugerPrime Upgrade [2] is ongoing. Based on the success of AERA [3], a main component is the Radio Detector (RD) [4]. Each WCD will be complemented by a radio antenna mounted on top which is sensitive to the electromagnetic (EM) component of the air shower. Especially, air showers with high zenith angles can then be detected, where the WCD is less sensitive to. This will increase the aperture of the observatory by $\approx 25\%$ and significantly increase the mass sensitive sky coverage [5].

2. Status of the Radio Detector

The design of the detector is a further developed antenna, originally designed for LOPES and used by AERA and Tunka-Rex [6], featuring two loop antennas with polarizations both parallel and perpendicular to Earth's magnetic field. The antenna can be seen in Fig. 1. The antenna arms, in combination with the loops, make the detector sensitive to electric fields in all directions, including the vertical component. This is particularly important as the antenna is designed to measure inclined air showers. Due to the large geometric distance with a lot of traversed mass from the shower maximum to the shower core on the ground, the electromagnetic (EM) component is already absorbed in the atmosphere, and only the muons reach the detectors, spread over a larger area. This renders the WCD less sensitive to inclined air showers. However, the RD still captures the radio emission produced at the shower maximum, making it a valuable addition to the WCD. Due to the great sensitivity to the EM component, an energy resolution better than 10 % is expected.

Since the radio footprints of inclined air showers can spread over large areas [7–9], the plan is to equip all WCDs with an antenna on top. With the array fully equipped, we expect more than 3 000 eventsabove 10 EeV within 10 years. The deployment is currently being carried out in two steps. Initially, the antenna is mounted together with the pre-amplifier, and the digitizer is installed at a later stage due to its delayed production date. As of 2023/07/12, **197** antennas have been deployed at a rate of approximately **8** additional antennas per working day. Among them, 38 have a digitizer installed (two central stations at the same location and three rings of stations around them). The area covered by these stations is approximately $70\,\mathrm{km}^2$, making the RD currently four times larger than AERA and the largest cosmic-ray radio detector worldwide. The digitizers for the remaining array will be delivered later in larger batches and each can be installed within minutes. Therefore, it is estimated that the deployment will be completed in early 2024.

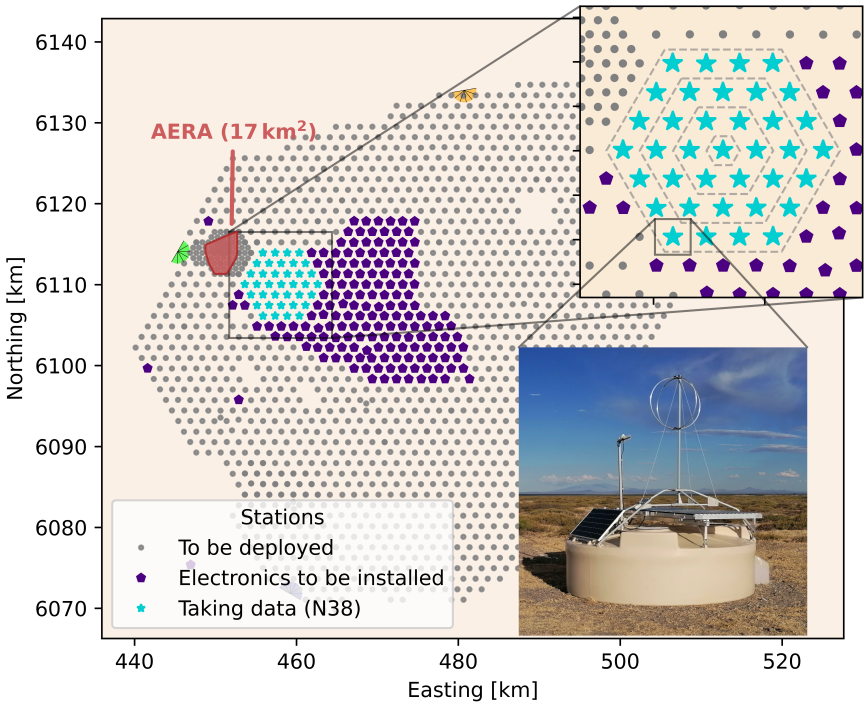

Figure 1: (Large image): the status of the deployment. The blue stars indicate the stations that are fully functional and taking data. The purple pentagons are the stations with mounted antenna but missing electronics. The grey points are the stations that still have to be equipped. For comparison, the area of AERA is sketched. (Upper right image): Zoom of the measuring stations. Two central stations with three rings (36 stations) around them. (Lower right image): Picture of a WCD with mounted antenna.

The deployment of the 38 functional stations was carried out in two phases. The central stations and the innermost ring of stations (8 stations) have been operational since 2019 and served as a test array. Since March 2023, they have been in a stable configuration. In June 2023, the two outer rings were added. Since the quality of reconstruction depends on the number of signal stations, the following differentiation will be made between these two phases, indicated by the abbreviations N8 and N38.

3. Measurement of cosmic rays

Despite the limited number of data-taking stations, the RD has already detected air showers with large radio footprints. Figure 2 illustrates an example event, demonstrating the information obtained from the air shower through the RD. The air shower was observed by five triggered WCDs, where the RD had a maximum energy fluence of approximately 1 600 eV/m^2, indicated by the size of the data points. The color coding provides information about the timing of the signal at each respective station, allowing for estimation of the arrival direction of the air shower. In this particular event, the air shower arrives from near south with a zenith angle of 72.5°. By combining the signal strengths at the signal stations and the arrival direction, an energy estimation (see also Sec. 4) of 11.6 EeV is obtained.

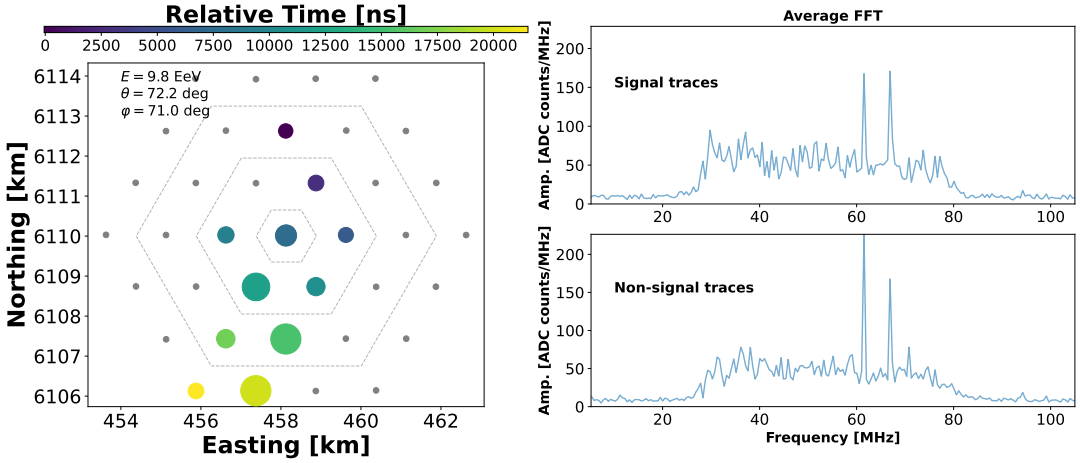

Figure 2: An example air shower is shown. (Left): Measured radio footprint of the air shower. Each dot represents one detector stations, the colors indicate the arrival times, while the size represents the signal strength. (Right): The average frequency spectrum of the event in case of a signal in the trace (top) and no signal in the trace (bottom) is shown.

Another intriguing aspect is the measured frequency spectrum. The right side of the figure displays the spectrum for cases with a signal and without a signal in the trace. Both spectra are clearly defined by the bandpass filter, which suppresses frequencies outside the range of 30 MHz to 80 MHz. Within this band, the amplitudes of different frequencies are stronger and remain consistent. In the presence of a signal, the amplitude is approximately 1.5 times higher than in the no-signal case. The background, seen in the non-signal traces, is featureless besides certain peaking frequencies. They can be attributed to known sources and suppressed during the reconstruction process. An example is the 67 MHz line originating from a TV station. Overall, the frequency spectrum exhibits the expected characteristics, with a well-defined sensitive band and amplitude dependent on the air shower signal. This provides a foundation for reconstructing these air showers on a large scale.

4. Hybrid measurement of events

The RD is sensitive to the EM-component of the shower and is therefore ideal to reconstruct the EM-energy of the air shower. This can be done by fitting the Lateral Distribution Function (LDF). Here, we take the calculated station distance to the shower axis r and the reconstructed geomagnetic station energy fluence f_{geo} and fit an empirical function [10] to it:

$$f_{\text{geo}}(r) = f_0 \left[\exp\left(-\left(\frac{r - r_0}{\sigma} \right)^p \right) + \frac{a_{\text{rel}}}{1 + \exp(s \cdot [r/r_0 - r_{02}])} \right], \tag{1}$$

where f_0 and the shower core coodinates are free parameters and $r_0, \sigma, p, a_{\text{rel}}, s$ and r_{02} are shape parameters fixed by the estimated shower maximum. An exemplary LDF fit is depicted as an inset of Fig. 3. With the shape parameters and the integration of the curve (see [10]) one gets the EM-energy of the air shower. Besides shower-to-shower fluctuations and a dependency on the primary particle composition, this energy is then correlated to the primary energy of the CR.

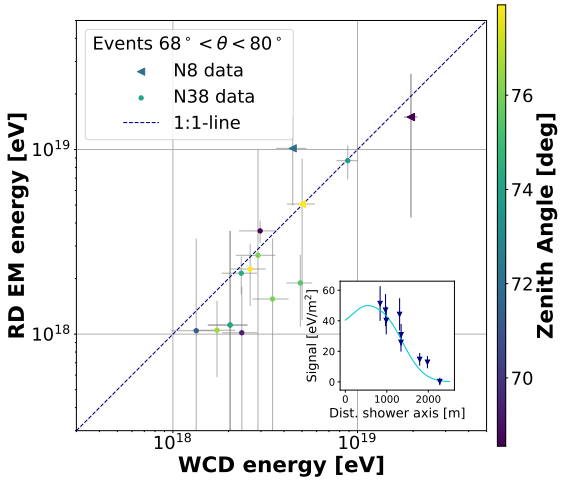

Figure 3: Comparison of the estimated energy of the particle detector and EM energy of the RD. Air showers are separated in N8 (triangles) and N38 (points) data. The color scale indicates the reconstructed zenith angle.

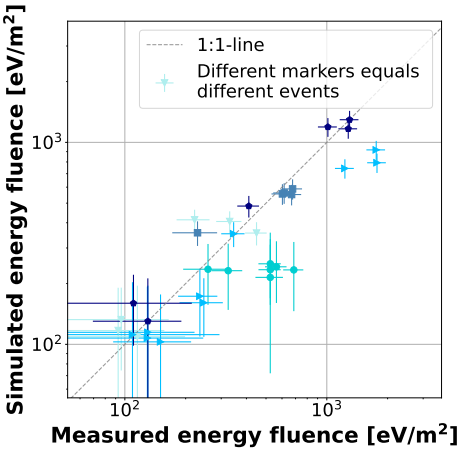

Figure 4: Comparison of measured and simulated signals. Each point is the mean of ten simulations for this station, the different colors and markers indicate the different events used.

As previously mentioned, the RD is most sensitive for inclined air showers, especially for zenith angles between 65° and 85°, while the WCDs are sensitive for more vertical events. Nonetheless, they have an overlap where both their reconstructions should be reliable and accurate. We can compare the calculated and long established energy estimation of the WCDs with an estimate of the EM-energy by the RD. This can be seen in Fig. 3. Each data point represents one reconstructed air shower, the colors indicate the reconstructed zenith angle. An event selection was done, requiring at least one radio station within a signal-to-noise ratio of 10 within 1.5 Cherenkov-radii. In addition at least 5 signal stations should be available for both RD and WCD. One observes a good agreement between both reconstructions, which is expected as the EM-part contributes the most to the shower. The result is satisfactory for the amount of stations existing, and a larger containment of the radio footprint will probably lead to even better results. This will likely decrease the uncertainty of the RD estimation too, as more signal stations would reduce the fit uncertainty. Additionally, a self standing radio geometry reconstruction (which is only possible with the containment of the radio core) would improve this aspect.

5. Comparison of measurements with simulations

The comparison of the RD energy reconstruction with the WCD demonstrates a good understanding of the reconstruction. However, maybe equally important, is the understanding of the detector itself. Especially being able to simulate a proper detector response across the whole range of detected signal strengths is of importance. For this purpose, we compare the measurements of various air showers of high reconstruction quality with simulations done with CoREAS [11]. Every air shower was taken ten times and a Gaussian smearing was applied each time to the reconstructed air shower (primary energy, zenith angle, azimuth angle), which corresponds to the uncertainty

of the WCD reconstruction (see Tab. 1). We then simulate the detector response with the Pierre Auger analysis framework, $\overline{\text{Off}}\underline{\text{line}}$ [12]. The comparison of the measured and simulated signals is shown in Fig. 4, where each point represents the mean of one detector station. The distance to the gray dashed line serves as an evaluation of how well our detector is described in the simulations. Deviations from the line can result from biases in the shower reconstruction where especially the core position has a major effect, statistical uncertainties, and uncertainties in the detector description. It is also notable that these factors can compensate each other. Nonetheless, the plot gives the impression that an accurate detector description is given. The simulated signals are in good agreement with the measured signals. Larger deviations seem to be grouped event wise, which indicates biases in the shower reconstruction and simulation settings. Small improvements to the detector description are in progress to further improve the result.

Table 1: Air shower geometries used for Fig. 4.

Energy [EeV]	Zenith angle [°]	Marker in plot
1.34 ± 0.37	70.7 ± 0.4	Downward triangle
2.62 ± 0.56	78.5 ± 0.2	Squares
4.90 ± 0.78	75.6 ± 0.2	Pentagons
8.21 ± 0.97	71.6 ± 0.2	Right triangles
1.88 ± 0.55	82.9 ± 0.6	Circles

6. Development of an RD trigger

One of the goals of the AugerPrime Upgrade is to increase sensitivity to UHE neutral particles, which would directly pinpoint their respective sources. The detection of such induced air showers would be a major achievement and could help solve puzzles like the unknown source of UHE particles. Here, the RD could play a key role in measuring and precisely reconstructing these events. In particular, UHE photons produce nearly pure EM showers, but neutrinos could also result in such showers. In the case of an inclined neutral air shower, the EM particles are absorbed in the atmosphere before reaching the ground, and only a few muons can reach particle detectors on the surface. Nonetheless, the radio signal remains strong as it is not absorbed and can travel hundreds of kilometers through the air. Hence, detection and accurate reconstruction are still possible. These circumstances come with the downside that one measures in the regime, where WCDs or other particle detectors in general are less sensitive to trigger neutral air showers. A stand-alone solution using radio detectors is needed.

Since there are no existing triggers that fulfill the requirements, a new trigger is under development that solely relies on the radio signal measured by the stations. The trigger fits into the general scheme of the Pierre Auger Observatory's triggering system [13], which will be briefly outlined here. First, the stations individually send out low-level triggers to the central triggering system when a specific threshold for the radio signal is reached (additional vetoing mechanisms, such as checking for air shower-like structures, are also used). Afterwards, the central triggering system decides, based on 3-fold coincidence of stations and fulfilling various other physics conditions, whether to save the data from the stations as an event.

From the beginning of 2023 to March 2023 (only during the N8 configuration), we tested the RD trigger and evaluated the data. Several events were measured that were only triggered by the RD and had no particle trigger contribution. Figure 5 shows an exemplary event of this kind. All signals measured in this event exhibit an air shower-like structure. It should be clarified that these events can still be caused by noise that triggered the stations, as there is no significant particle signal seen in the WCD, and some sources can cause such signals. Although the source remains uncertain and no reliable reconstruction of the measured events is possible, the test can be evaluated as successful since air shower-like events were measured and the background trigger rate was acceptable. The trigger is still under further development, and it is promising that it can be implemented for all stations in the future.

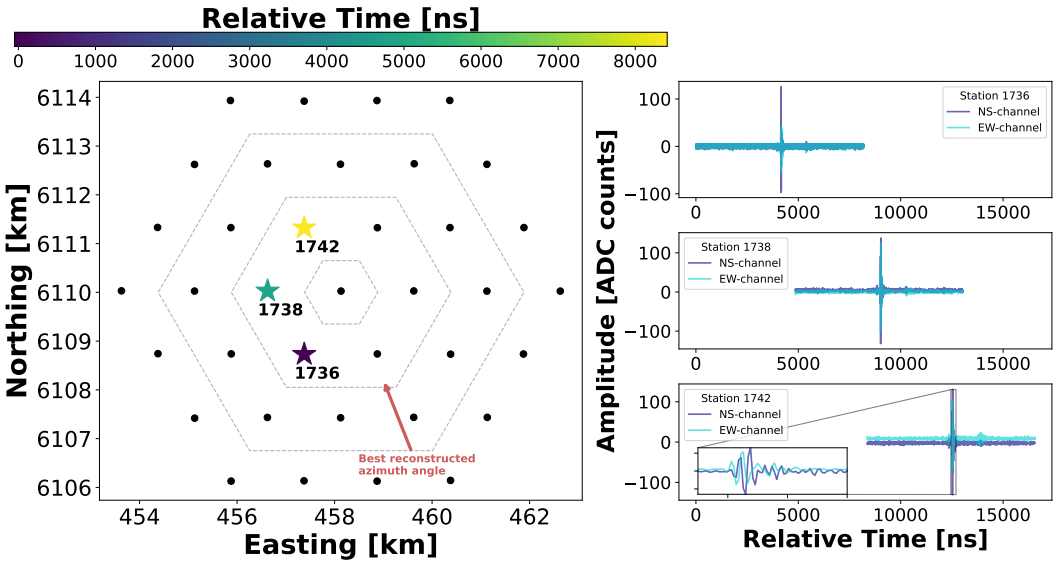

Figure 5: (Left): Map of the RD triggered stations. The color code indicates the time of the signal. (Right): Measured signals for both polarization and different stations. All signals show air shower like structure.

In addition to the hardware implementation, the effect of the trigger was also simulated [14]. We simulated a broad range of air showers with CoREAS and reconstructed them in $\overline{\text{Off}}\underline{\text{line}}$. A version of the trigger with an optimistic threshold of 25 ADC counts was applied to the CoREAS simulations, and the detector response was evaluated. A threshold of 25 ADC counts is one of the lowest values that the trigger can have while still being compatible with hardware limitations like the maximum bandwidth of data transfer. The major limiting factor is the noise level, which is in the order of a few ADC counts. The results are shown in Fig. 6. It can be observed that including the RD trigger leads to a significant increase in the trigger probability for all investigated zenith angle ranges compared to using only particle triggers. The same trend is visible for the energy dependence, except for the combination of the lowest zenith angle range and energy bins where no significant increase is obtained. The weighted trigger efficiency (following an E^{-2} energy spectrum) increases by almost a factor of four, from approximately 12 % to 46 %. For a more conservative trigger threshold of 60 ADC counts, the trigger probability doubles from 12 % to 25 %.

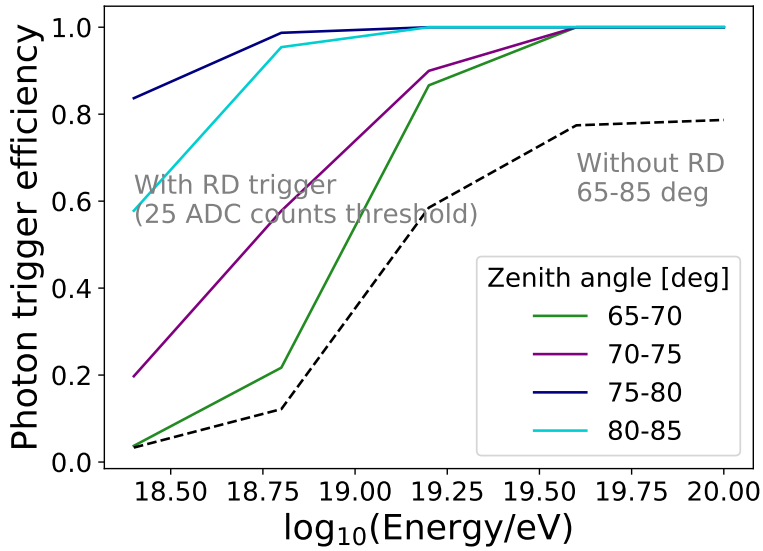

Figure 6: Shown is the simulated photon trigger efficiency with implemented RD trigger with 25 ADC counts trigger threshold for different energy bins. The colors indicate the investigated zenith angle range, the dashed line represents the current setup without an RD trigger.

7. Conclusion

We have presented the status and progress of the RD of the AugerPrime Upgrade. We have shown that significant progress was made to ensure a fast deployment and reliable data taking. First results of the measurements indicate a good understanding of the detector and results comparable to the other detectors at the observatory. Additionally, we gave an outlook on developing a stand-alone RD trigger. This will make the RD even more sensitive to neutral cosmic rays.

References

[1] T. Huege for the Pierre Auger Collaboration, EPJ Web of Conf. (2019), 210:05011
[2] A.Aab et al. [Pierre Auger Collaboration], arXiv:1604.03637 (2016)
[3] M. Gottowik for the Pierre Auger Collaboration, PoS(ICRC2019) (2019) 274
[4] J. R. Hörandel for the Pierre Auger Collaboration, EPJ Web of Conf. (2019), 210:06005
[5] F. Schlüter for the Pierre Auger Collaboration, PoS(ARENA2022) (2022) 028
[6] R. Hiller et al., ICRC 2013, 1278
[7] F. Schlüter et al., EPJ C (2020),80: 643
[8] T. Huege, A. Haungs, JPS Conf. Proc. 9, 010018 (2016)
[9] M. Gottowik for the Pierre Auger Collaboration, EPJ Web of Conf. (2019), 216:02001
[10] F. Schlüter, T. Huege, 10.1088/1475-7516/2023/01/008 (2023)
[11] T. Huege et al., AIP Conf. Proc. 1535 128 (2013)
[12] S. Argiro et al., Nucl. Instrum. Meth. A 580 (2004), 1485 [0707.1652]
[13] R. Sato for the Pierre Auger Collaboration, PoS(ICRC2023) (2023) 373
[14] J. Pawlowsky for the Pierre Auger Collaboration, PoS(ARENA2022) (2022) 054

The Pierre Auger Collaboration

A. Abdul Halim[13], P. Abreu[72], M. Aglietta[54,52], I. Allekotte[1], K. Almeida Cheminant[70], A. Almela[7,12], R. Aloisio[45,46], J. Alvarez-Muñiz[79], J. Ammerman Yebra[79], G.A. Anastasi[54,52], L. Anchordoqui[86], B. Andrada[7], S. Andringa[72], C. Aramo[50], P.R. Araújo Ferreira[42], E. Arnone[63,52], J. C. Arteaga Velázquez[67], H. Asorey[7], P. Assis[72], G. Avila[11], E. Avocone[57,46], A.M. Badescu[75], A. Bakalova[32], A. Balaceanu[73], F. Barbato[45,46], A. Bartz Mocellin[85], J.A. Bellido[13,69], C. Berat[36], M.E. Bertaina[63,52], G. Bhatta[70], M. Bianciotto[63,52], P.L. Biermann[h], V. Binet[5], K. Bismark[39,7], T. Bister[80,81], J. Biteau[37], J. Blazek[32], C. Bleve[36], J. Blümer[41], M. Boháčová[32], D. Boncioli[57,46], C. Bonifazi[8,26], L. Bonneau Arbeletche[21], N. Borodai[70], J. Brack[j], P.G. Brichetto Orchera[7], F.L. Briechle[42], A. Bueno[78], S. Buitink[15], M. Buscemi[47,61], M. Büsken[39,7], A. Bwembya[80,81], K.S. Caballero-Mora[66], S. Cabana-Freire[79], L. Caccianiga[59,49], I. Caracas[38], R. Caruso[58,47], A. Castellina[54,52], F. Catalani[18], G. Cataldi[48], L. Cazon[79], M. Cerda[10], A. Cermenati[45,46], J.A. Chinellato[21], J. Chudoba[32], L. Chytka[33], R.W. Clay[13], A.C. Cobos Cerutti[6], R. Colalillo[60,50], A. Coleman[90], M.R. Coluccia[48], R. Conceição[72], A. Condorelli[37], G. Consolati[49,55], M. Conte[56,48], F. Convenga[41], D. Correia dos Santos[28], P.J. Costa[72], C.E. Covault[84], M. Cristinziani[44], C.S. Cruz Sanchez[3], S. Dasso[4,2], K. Daumiller[41], B.R. Dawson[13], R.M. de Almeida[28], J. de Jesús[7,41], S.J. de Jong[80,81], J.R.T. de Mello Neto[26,27], I. De Mitri[45,46], J. de Oliveira[17], D. de Oliveira Franco[21], F. de Palma[56,48], V. de Souza[19], E. De Vito[56,48], A. Del Popolo[58,47], O. Deligny[34], N. Denner[32], L. Deval[41,7], A. di Matteo[52], M. Dobre[73], C. Dobrigkeit[21], J.C. D'Olivo[68], L.M. Domingues Mendes[72], J.C. dos Anjos, R.C. dos Anjos[25], J. Ebr[32], F. Ellwanger[41], M. Emam[80,81], R. Engel[39,41], I. Epicoco[56,48], M. Erdmann[42], A. Etchegoyen[7,12], C. Evoli[45,46], H. Falcke[80,82,81], J. Farmer[89], G. Farrar[88], A.C. Fauth[21], N. Fazzini[e], F. Feldbusch[40], F. Fenu[41,d], A. Fernandes[72], B. Fick[87], J.M. Figueira[7], A. Filipčič[77,76], T. Fitoussi[41], B. Flaggs[90], T. Fodran[80], T. Fujii[89,f], A. Fuster[7,12], C. Galea[80], C. Galelli[59,49], B. García[6], C. Gaudu[38], H. Gemmeke[40], F. Gesualdi[7,41], A. Gherghel-Lascu[73], P.L. Ghia[34], U. Giaccari[48], M. Giammarchi[49], J. Glombitza[42,g], F. Gobbi[10], F. Gollan[7], G. Golup[1], M. Gómez Berisso[1], P.F. Gómez Vitale[11], J.P. Gongora[11], J.M. González[1], N. González[7], I. Goos[1], D. Góra[70], A. Gorgi[54,52], M. Gottowik[79], T.D. Grubb[13], F. Guarino[60,50], G.P. Guedes[22], E. Guido[44], S. Hahn[39], P. Hamal[32], M.R. Hampel[7], P. Hansen[3], D. Harari[1], V.M. Harvey[13], A. Haungs[41], T. Hebbeker[42], C. Hojvat[e], J.R. Hörandel[80,81], P. Horvath[33], M. Hrabovský[33], T. Huege[41,15], A. Insolia[58,47], P.G. Isar[74], P. Janecek[32], J.A. Johnsen[85], J. Jurysek[32], A. Kääpä[38], K.H. Kampert[38], B. Keilhauer[41], A. Khakurdikar[80], V.V. Kizakke Covilakam[7,41], H.O. Klages[41], M. Kleifges[40], F. Knapp[39], N. Kunka[40], B.L. Lago[16], N. Langner[42], M.A. Leigui de Oliveira[24], Y Lema-Capeans[79], V. Lenok[39], A. Letessier-Selvon[35], I. Lhenry-Yvon[34], D. Lo Presti[58,47], L. Lopes[72], L. Lu[91], Q. Luce[39], J.P. Lundquist[76], A. Machado Payeras[21], M. Majercakova[32], D. Mandat[32], B.C. Manning[13], P. Mantsch[e], S. Marafico[34], F.M. Mariani[59,49], A.G. Mariazzi[3], I.C. Mariş[14], G. Marsella[61,47], D. Martello[56,48], S. Martinelli[41,7], O. Martínez Bravo[64], M.A. Martins[79], M. Mastrodicasa[57,46], H.J. Mathes[41], J. Matthews[a], G. Matthiae[62,51], E. Mayotte[85,38], S. Mayotte[85], P.O. Mazur[e], G. Medina-Tanco[68], J. Meinert[38], D. Melo[7], A. Menshikov[40], C. Merx[41], S. Michal[33], M.I. Micheletti[5], L. Miramonti[59,49], S. Mollerach[1], F. Montanet[36], L. Morejon[38], C. Morello[54,52], A.L. Müller[32], K. Mulrey[80,81], R. Mussa[52], M. Muzio[88], W.M. Namasaka[38], S. Negi[32], L. Nellen[68], K. Nguyen[87], G. Nicora[9], M. Niculescu-Oglinzanu[73], M. Niechciol[44], D. Nitz[87], D. Nosek[31], V. Novotny[31], L. Nožka[33], A Nucita[56,48], L.A. Núñez[30], C. Oliveira[19], M. Palatka[32], J. Pallotta[9], S. Panja[32], G. Parente[79], T. Paulsen[38], J. Pawlowsky[38], M. Pech[32], J. Pękala[70], R. Pelayo[65], L.A.S. Pereira[23], E.E. Pereira Martins[39,7], J. Perez Armand[20], C. Pérez Bertolli[7,41], L. Perrone[56,48], S. Petrera[45,46], C. Petrucci[57,46], T. Pierog[41], M. Pimenta[72], M. Platino[7], B. Pont[80], M. Pothast[81,80], M. Pourmohammad Shahvar[61,47], P. Privitera[89], M. Prouza[32], A. Puyleart[87], S. Querchfeld[38], J. Rautenberg[38], D. Ravignani[7], M. Reininghaus[39], J. Ridky[32], F. Riehn[79], M. Risse[44], V. Rizi[57,46], W. Rodrigues de Carvalho[80], E. Rodriguez[7,41], J. Rodriguez Rojo[11], M.J. Roncoroni[7], S. Rossoni[43], M. Roth[41], E. Roulet[1], A.C. Rovero[4], P. Ruehl[44], A. Saftoiu[73], M. Saharan[80], F. Salamida[57,46], H. Salazar[64], G. Salina[51], J.D. Sanabria Gomez[30], F. Sánchez[7], E.M. Santos[20], E. Santos[32],

F. Sarazin[85], R. Sarmento[72], R. Sato[11], P. Savina[91], C.M. Schäfer[41], V. Scherini[56,48], H. Schieler[41], M. Schimassek[34], M. Schimp[38], F. Schlüter[41], D. Schmidt[39], O. Scholten[15,i], H. Schoorlemmer[80,81], P. Schovánek[32], F.G. Schröder[90,41], J. Schulte[42], T. Schulz[41], S.J. Sciutto[3], M. Scornavacche[7,41], A. Segreto[53,47], S. Sehgal[38], S.U. Shivashankara[76], G. Sigl[43], G. Silli[7], O. Sima[73,b], F. Simon[40], R. Smau[73], R. Šmída[89], P. Sommers[k], J.F. Soriano[86], R. Squartini[10], M. Stadelmaier[32], D. Stanca[73], S. Stanič[76], J. Stasielak[70], P. Stassi[36], S. Strähnz[39], M. Straub[42], M. Suárez-Durán[14], T. Suomijärvi[37], A.D. Supanitsky[7], Z. Svozilikova[32], Z. Szadkowski[71], A. Tapia[29], C. Taricco[63,52], C. Timmermans[81,80], O. Tkachenko[41], P. Tobiska[32], C.J. Todero Peixoto[18], B. Tomé[72], Z. Torrès[36], A. Travaini[10], P. Travnicek[32], C. Trimarelli[57,46], M. Tueros[3], M. Unger[41], L. Vaclavek[33], M. Vacula[33], J.F. Valdés Galicia[68], L. Valore[60,50], E. Varela[64], A. Vásquez-Ramírez[30], D. Veberič[41], C. Ventura[27], I.D. Vergara Quispe[3], V. Verzi[51], J. Vicha[32], J. Vink[83], J. Vlastimil[32], S. Vorobiov[76], C. Watanabe[26], A.A. Watson[c], A. Weindl[41], L. Wiencke[85], H. Wilczyński[70], D. Wittkowski[38], B. Wundheiler[7], B. Yue[38], A. Yushkov[32], O. Zapparrata[14], E. Zas[79], D. Zavrtanik[76,77], M. Zavrtanik[77,76]

[1] Centro Atómico Bariloche and Instituto Balseiro (CNEA-UNCuyo-CONICET), San Carlos de Bariloche, Argentina
[2] Departamento de Física and Departamento de Ciencias de la Atmósfera y los Océanos, FCEyN, Universidad de Buenos Aires and CONICET, Buenos Aires, Argentina
[3] IFLP, Universidad Nacional de La Plata and CONICET, La Plata, Argentina
[4] Instituto de Astronomía y Física del Espacio (IAFE, CONICET-UBA), Buenos Aires, Argentina
[5] Instituto de Física de Rosario (IFIR) – CONICET/U.N.R. and Facultad de Ciencias Bioquímicas y Farmacéuticas U.N.R., Rosario, Argentina
[6] Instituto de Tecnologías en Detección y Astropartículas (CNEA, CONICET, UNSAM), and Universidad Tecnológica Nacional – Facultad Regional Mendoza (CONICET/CNEA), Mendoza, Argentina
[7] Instituto de Tecnologías en Detección y Astropartículas (CNEA, CONICET, UNSAM), Buenos Aires, Argentina
[8] International Center of Advanced Studies and Instituto de Ciencias Físicas, ECyT-UNSAM and CONICET, Campus Miguelete – San Martín, Buenos Aires, Argentina
[9] Laboratorio Atmósfera – Departamento de Investigaciones en Láseres y sus Aplicaciones – UNIDEF (CITEDEF-CONICET), Argentina
[10] Observatorio Pierre Auger, Malargüe, Argentina
[11] Observatorio Pierre Auger and Comisión Nacional de Energía Atómica, Malargüe, Argentina
[12] Universidad Tecnológica Nacional – Facultad Regional Buenos Aires, Buenos Aires, Argentina
[13] University of Adelaide, Adelaide, S.A., Australia
[14] Université Libre de Bruxelles (ULB), Brussels, Belgium
[15] Vrije Universiteit Brussels, Brussels, Belgium
[16] Centro Federal de Educação Tecnológica Celso Suckow da Fonseca, Petropolis, Brazil
[17] Instituto Federal de Educação, Ciência e Tecnologia do Rio de Janeiro (IFRJ), Brazil
[18] Universidade de São Paulo, Escola de Engenharia de Lorena, Lorena, SP, Brazil
[19] Universidade de São Paulo, Instituto de Física de São Carlos, São Carlos, SP, Brazil
[20] Universidade de São Paulo, Instituto de Física, São Paulo, SP, Brazil
[21] Universidade Estadual de Campinas, IFGW, Campinas, SP, Brazil
[22] Universidade Estadual de Feira de Santana, Feira de Santana, Brazil
[23] Universidade Federal de Campina Grande, Centro de Ciencias e Tecnologia, Campina Grande, Brazil
[24] Universidade Federal do ABC, Santo André, SP, Brazil
[25] Universidade Federal do Paraná, Setor Palotina, Palotina, Brazil
[26] Universidade Federal do Rio de Janeiro, Instituto de Física, Rio de Janeiro, RJ, Brazil
[27] Universidade Federal do Rio de Janeiro (UFRJ), Observatório do Valongo, Rio de Janeiro, RJ, Brazil
[28] Universidade Federal Fluminense, EEIMVR, Volta Redonda, RJ, Brazil
[29] Universidad de Medellín, Medellín, Colombia
[30] Universidad Industrial de Santander, Bucaramanga, Colombia

[31] Charles University, Faculty of Mathematics and Physics, Institute of Particle and Nuclear Physics, Prague, Czech Republic
[32] Institute of Physics of the Czech Academy of Sciences, Prague, Czech Republic
[33] Palacky University, Olomouc, Czech Republic
[34] CNRS/IN2P3, IJCLab, Université Paris-Saclay, Orsay, France
[35] Laboratoire de Physique Nucléaire et de Hautes Energies (LPNHE), Sorbonne Université, Université de Paris, CNRS-IN2P3, Paris, France
[36] Univ. Grenoble Alpes, CNRS, Grenoble Institute of Engineering Univ. Grenoble Alpes, LPSC-IN2P3, 38000 Grenoble, France
[37] Université Paris-Saclay, CNRS/IN2P3, IJCLab, Orsay, France
[38] Bergische Universität Wuppertal, Department of Physics, Wuppertal, Germany
[39] Karlsruhe Institute of Technology (KIT), Institute for Experimental Particle Physics, Karlsruhe, Germany
[40] Karlsruhe Institute of Technology (KIT), Institut für Prozessdatenverarbeitung und Elektronik, Karlsruhe, Germany
[41] Karlsruhe Institute of Technology (KIT), Institute for Astroparticle Physics, Karlsruhe, Germany
[42] RWTH Aachen University, III. Physikalisches Institut A, Aachen, Germany
[43] Universität Hamburg, II. Institut für Theoretische Physik, Hamburg, Germany
[44] Universität Siegen, Department Physik – Experimentelle Teilchenphysik, Siegen, Germany
[45] Gran Sasso Science Institute, L'Aquila, Italy
[46] INFN Laboratori Nazionali del Gran Sasso, Assergi (L'Aquila), Italy
[47] INFN, Sezione di Catania, Catania, Italy
[48] INFN, Sezione di Lecce, Lecce, Italy
[49] INFN, Sezione di Milano, Milano, Italy
[50] INFN, Sezione di Napoli, Napoli, Italy
[51] INFN, Sezione di Roma "Tor Vergata", Roma, Italy
[52] INFN, Sezione di Torino, Torino, Italy
[53] Istituto di Astrofisica Spaziale e Fisica Cosmica di Palermo (INAF), Palermo, Italy
[54] Osservatorio Astrofisico di Torino (INAF), Torino, Italy
[55] Politecnico di Milano, Dipartimento di Scienze e Tecnologie Aerospaziali , Milano, Italy
[56] Università del Salento, Dipartimento di Matematica e Fisica "E. De Giorgi", Lecce, Italy
[57] Università dell'Aquila, Dipartimento di Scienze Fisiche e Chimiche, L'Aquila, Italy
[58] Università di Catania, Dipartimento di Fisica e Astronomia "Ettore Majorana", Catania, Italy
[59] Università di Milano, Dipartimento di Fisica, Milano, Italy
[60] Università di Napoli "Federico II", Dipartimento di Fisica "Ettore Pancini", Napoli, Italy
[61] Università di Palermo, Dipartimento di Fisica e Chimica "E. Segrè", Palermo, Italy
[62] Università di Roma "Tor Vergata", Dipartimento di Fisica, Roma, Italy
[63] Università Torino, Dipartimento di Fisica, Torino, Italy
[64] Benemérita Universidad Autónoma de Puebla, Puebla, México
[65] Unidad Profesional Interdisciplinaria en Ingeniería y Tecnologías Avanzadas del Instituto Politécnico Nacional (UPIITA-IPN), México, D.F., México
[66] Universidad Autónoma de Chiapas, Tuxtla Gutiérrez, Chiapas, México
[67] Universidad Michoacana de San Nicolás de Hidalgo, Morelia, Michoacán, México
[68] Universidad Nacional Autónoma de México, México, D.F., México
[69] Universidad Nacional de San Agustin de Arequipa, Facultad de Ciencias Naturales y Formales, Arequipa, Peru
[70] Institute of Nuclear Physics PAN, Krakow, Poland
[71] University of Łódź, Faculty of High-Energy Astrophysics,Łódź, Poland
[72] Laboratório de Instrumentação e Física Experimental de Partículas – LIP and Instituto Superior Técnico – IST, Universidade de Lisboa – UL, Lisboa, Portugal
[73] "Horia Hulubei" National Institute for Physics and Nuclear Engineering, Bucharest-Magurele, Romania
[74] Institute of Space Science, Bucharest-Magurele, Romania
[75] University Politehnica of Bucharest, Bucharest, Romania
[76] Center for Astrophysics and Cosmology (CAC), University of Nova Gorica, Nova Gorica, Slovenia
[77] Experimental Particle Physics Department, J. Stefan Institute, Ljubljana, Slovenia

[78] Universidad de Granada and C.A.F.P.E., Granada, Spain
[79] Instituto Galego de Física de Altas Enerxías (IGFAE), Universidade de Santiago de Compostela, Santiago de Compostela, Spain
[80] IMAPP, Radboud University Nijmegen, Nijmegen, The Netherlands
[81] Nationaal Instituut voor Kernfysica en Hoge Energie Fysica (NIKHEF), Science Park, Amsterdam, The Netherlands
[82] Stichting Astronomisch Onderzoek in Nederland (ASTRON), Dwingeloo, The Netherlands
[83] Universiteit van Amsterdam, Faculty of Science, Amsterdam, The Netherlands
[84] Case Western Reserve University, Cleveland, OH, USA
[85] Colorado School of Mines, Golden, CO, USA
[86] Department of Physics and Astronomy, Lehman College, City University of New York, Bronx, NY, USA
[87] Michigan Technological University, Houghton, MI, USA
[88] New York University, New York, NY, USA
[89] University of Chicago, Enrico Fermi Institute, Chicago, IL, USA
[90] University of Delaware, Department of Physics and Astronomy, Bartol Research Institute, Newark, DE, USA
[91] University of Wisconsin-Madison, Department of Physics and WIPAC, Madison, WI, USA

—

[a] Louisiana State University, Baton Rouge, LA, USA
[b] also at University of Bucharest, Physics Department, Bucharest, Romania
[c] School of Physics and Astronomy, University of Leeds, Leeds, United Kingdom
[d] now at Agenzia Spaziale Italiana (ASI). Via del Politecnico 00133, Roma, Italy
[e] Fermi National Accelerator Laboratory, Fermilab, Batavia, IL, USA
[f] now at Graduate School of Science, Osaka Metropolitan University, Osaka, Japan
[g] now at ECAP, Erlangen, Germany
[h] Max-Planck-Institut für Radioastronomie, Bonn, Germany
[i] also at Kapteyn Institute, University of Groningen, Groningen, The Netherlands
[j] Colorado State University, Fort Collins, CO, USA
[k] Pennsylvania State University, University Park, PA, USA

Acknowledgments

The successful installation, commissioning, and operation of the Pierre Auger Observatory would not have been possible without the strong commitment and effort from the technical and administrative staff in Malargüe. We are very grateful to the following agencies and organizations for financial support:

Argentina – Comisión Nacional de Energía Atómica; Agencia Nacional de Promoción Científica y Tecnológica (ANPCyT); Consejo Nacional de Investigaciones Científicas y Técnicas (CONICET); Gobierno de la Provincia de Mendoza; Municipalidad de Malargüe; NDM Holdings and Valle Las Leñas; in gratitude for their continuing cooperation over land access; Australia – the Australian Research Council; Belgium – Fonds de la Recherche Scientifique (FNRS); Research Foundation Flanders (FWO); Brazil – Conselho Nacional de Desenvolvimento Científico e Tecnológico (CNPq); Financiadora de Estudos e Projetos (FINEP); Fundação de Amparo à Pesquisa do Estado de Rio de Janeiro (FAPERJ); São Paulo Research Foundation (FAPESP) Grants No. 2019/10151-2, No. 2010/07359-6 and No. 1999/05404-3; Ministério da Ciência, Tecnologia, Inovações e Comunicações (MCTIC); Czech Republic – Grant No. MSMT CR LTT18004, LM2015038, LM2018102, CZ.02.1.01/0.0/0.0/16_013/0001402, CZ.02.1.01/0.0/0.0/18_046/0016010 and CZ.02.1.01/0.0/0.0/17_049/0008422; France – Centre de Calcul IN2P3/CNRS; Centre National de la Recherche Scientifique (CNRS); Conseil Régional Ile-de-France; Département Physique Nucléaire et Corpusculaire (PNC-IN2P3/CNRS); Département Sciences de l'Univers (SDU-INSU/CNRS); Institut Lagrange de Paris (ILP) Grant No. LABEX ANR-10-LABX-63 within the Investissements d'Avenir Programme Grant No. ANR-11-IDEX-0004-02; Germany – Bundesministerium für Bildung und Forschung (BMBF); Deutsche Forschungsgemeinschaft (DFG); Finanzministerium Baden-Württemberg; Helmholtz Alliance for Astroparticle Physics (HAP); Helmholtz-Gemeinschaft Deutscher Forschungszentren (HGF); Ministerium für Kultur und Wissenschaft des Landes Nordrhein-Westfalen; Ministerium für Wissenschaft, Forschung und Kunst des Landes Baden-Württemberg; Italy – Istituto Nazionale di Fisica Nucleare (INFN); Istituto Nazionale di Astrofisica (INAF); Ministero dell'Istruzione, dell'Universitá e della Ricerca (MIUR); CETEMPS Center of Excellence; Ministero degli Affari Esteri (MAE), ICSC Centro Nazionale di Ricerca in High Performance Computing, Big Data and Quantum Computing, funded by European Union NextGenerationEU, reference code CN_00000013;

México – Consejo Nacional de Ciencia y Tecnología (CONACYT) No. 167733; Universidad Nacional Autónoma de México (UNAM); PAPIIT DGAPA-UNAM; The Netherlands – Ministry of Education, Culture and Science; Netherlands Organisation for Scientific Research (NWO); Dutch national e-infrastructure with the support of SURF Cooperative; Poland – Ministry of Education and Science, grants No. DIR/WK/2018/11 and 2022/WK/12; National Science Centre, grants No. 2016/22/M/ST9/00198, 2016/23/B/ST9/01635, 2020/39/B/ST9/01398, and 2022/45/B/ST9/02163; Portugal – Portuguese national funds and FEDER funds within Programa Operacional Factores de Competitividade through Fundação para a Ciência e a Tecnologia (COMPETE); Romania – Ministry of Research, Innovation and Digitization, CNCS-UEFISCDI, contract no. 30N/2023 under Romanian National Core Program LAPLAS VII, grant no. PN 23 21 01 02 and project number PN-III-P1-1.1-TE-2021-0924/TE57/2022, within PNCDI III; Slovenia – Slovenian Research Agency, grants P1-0031, P1-0385, I0-0033, N1-0111; Spain – Ministerio de Economía, Industria y Competitividad (FPA2017-85114-P and PID2019-104676GB-C32), Xunta de Galicia (ED431C 2017/07), Junta de Andalucía (SOMM17/6104/UGR, P18-FR-4314) Feder Funds, RENATA Red Nacional Temática de Astropartículas (FPA2015-68783-REDT) and María de Maeztu Unit of Excellence (MDM-2016-0692); USA – Department of Energy, Contracts No. DE-AC02-07CH11359, No. DE-FR02-04ER41300, No. DE-FG02-99ER41107 and No. DE-SC0011689; National Science Foundation, Grant No. 0450696; The Grainger Foundation; Marie Curie-IRSES/EPLANET; European Particle Physics Latin American Network; and UNESCO.